Received 29 March; accepted 25 June 2001.

1. Hyman, L. H. *The Invertebrates* Vol. 4 (McGraw-Hill, New York, 1955).
2. Millott, N. The photosensitivity of echinoids. *Adv. Mar. Biol.* **13,** 1–52 (1975).
3. Yoshida, M., Takasu, N. & Tamotsu, S. in *Photoreception and Vision in Invertebrates*; (ed. Ali, M. A.) 743–771 (Plenum, New York, 1984).
4. Lowenstam, H. A. & Weiner, S. *On Biomineralization* 123–134 (Oxford Univ. Press, Oxford, 1989).
5. Wainwright, S. A., Biggs, W. D., Currey, J. D. & Gosline, J. M. *Mechanical Design in Organisms* (John Wiley, New York, 1976).
6. Hendler, G. & Byrne, M. Fine structure of the dorsal arm plate of *Ophiocoma wendti* (Echinodermata, Ophiuroidea). *Zoomorphology* **107,** 261–272 (1987).
7. Hendler, G. Brittlestar color-change and phototaxis (Echinodermata: Ophiuroidea: Ophiocomidae). *Mar. Ecol.* **5,** 379–401 (1984).
8. Cowles, R. P. Stimuli produced by light and by contact with solid walls as factors in the behavior of ophiuroids. *J. Exp. Zool.* **9,** 387–416 (1910).
9. Donnay, G. & Pawson, D. L. X-ray diffraction studies of echinoderm plates. *Science* **166,** 1147–1150 (1969).
10. Ameye, L., Hermann, R., Wilt, F. & Dubois, P. Ultrastructural localization of proteins involved in sea urchin biomineralization. *J. Histochem. Cytochem.* **47,** 1189–1200 (1999).
11. Clarkson, E. N. K. & Levi-Setti, R. Trilobite eyes and the optics of Des Cartes and Huygens. *Nature* **254,** 663–667 (1975).
12. Gal, J., Horvath, G., Clarkson, E. N. K. & Haiman, O. Image formation by bifocal lenses in a trilobite eye? *Vision Res.* **40,** 843–853 (2000).
13. Towe, K. M. Trilobite eyes: calcified lenses *in vivo*. *Science* **179,** 1007–1010 (1973).
14. Döderlein, L. Ueber 'Krystallkörper' bei Seesternen. *Denkschr. Med. Nat. Ges. Jena* **8,** 491–494 (1898).
15. Smith, A. B. in *Special Papers in Palaeontology* **25,** 1–81 (Palaeontology Association, London, 1980).
16. Xia, Y. N. & Whitesides, G. M. Soft lithography. *Annu. Rev. Mater. Sci.* **28,** 153–184 (1998).
17. Aizenberg, J., Rogers, J. A., Paul, K. E. & Whitesides, G. M. Imaging the irradiance distribution in the optical near field. *Appl. Phys. Lett.* **71,** 3773–3775 (1997).
18. Flint, H. T. *Geometrical Optics* (Methuen, London, 1936).
19. Cobb, J. L. S. & Moore, A. Comparative studies on receptor structure in the brittlestar *Ophiura ophiura*. *J. Neurocytol.* **15,** 97–108 (1986).
20. Johnsen, S. Identification and localization of a possible rhodopsin in the echinoderms *Asterias forbesi* (Asteroidea) and *Ophioderma brevispinum* (Ophiuroidea). *Biol. Bull.* **193,** 97–105 (1997).
21. Cobb, J. L. S. & Hendler, G. Neurophysiological characterization of the photoreceptor system in brittlestars. *Comp. Biochem. Physiol.* **97A,** 329–333 (1990).
22. Stubbs, T. R. in *Echinoderms* (ed. Lawrence, J. M.) 403–408 (Proc. Int. Echinoderms Conf., Tampa Bay, 1982).
23. Land, M. F. in *Comparative Physiology and Evolution in Invertebrates B: Invertebrate Visual Centers and Behavior I* (ed. Autrum, H.) 471–592 (Springer, Berlin, 1981).
24. Mann, S. & Ozin, G. A. Synthesis of inorganic materials with complex form. *Nature* **382,** 313–318 (1996).
25. Belcher, A. M., Hansma, P. K., Stucky, G. D. & Morse, D. E. First steps in harnessing the potential of biomineralization. *Acta Mater.* **46,** 733–736 (1998).

Acknowledgements

We thank P. Wiltzius and M. Megens for helpful discussions.

Correspondence and requests for materials should be addressed to J.A. (e-mail: jaizenberg@lucent.com).

Delineation of prognostic biomarkers in prostate cancer

Saravana M. Dhanasekaran*, Terrence R. Barrette*, Debashis Ghosh†, Rajal Shah*, Sooryanarayana Varambally*, Kotoku Kurachi‡, Kenneth J. Pienta§‖¶, Mark A. Rubin*§¶# & Arul M. Chinnaiyan*§¶#

*Departments of * Pathology, † Biostatistics, ‡ Human Genetics, § Urology, ‖ Internal Medicine, and ¶ Comprehensive Cancer Center, University of Michigan Medical School, Ann Arbor, Michigan 48109, USA*
 # These authors share senior authorship

Prostate cancer is the most frequently diagnosed cancer in American men[1,2]. Screening for prostate-specific antigen (PSA) has led to earlier detection of prostate cancer[3], but elevated serum PSA levels may be present in non-malignant conditions such as benign prostatic hyperlasia (BPH). Characterization of gene-expression profiles that molecularly distinguish prostatic neoplasms may identify genes involved in prostate carcinogenesis, elucidate clinical biomarkers, and lead to an improved classification of prostate cancer[4–6]. Using microarrays of complementary DNA, we examined gene-expression profiles of more than 50 normal and neoplastic prostate specimens and three common prostate-cancer cell lines. Signature expression profiles of normal adjacent prostate (NAP), BPH, localized prostate cancer, and metastatic, hormone-refractory prostate cancer were determined. Here we establish many associations between genes and prostate cancer. We assessed two of these genes—hepsin, a transmembrane serine protease, and pim-1, a serine/threonine kinase—at the protein level using tissue microarrays consisting of over 700 clinically stratified prostate-cancer specimens. Expression of hepsin and pim-1 proteins was significantly correlated with measures of clinical outcome. Thus, the integration of cDNA microarray, high-density tissue microarray, and linked clinical and pathology data is a powerful approach to molecular profiling of human cancer.

We developed a 9,984-element (10K) human cDNA microarray to analyse gene expression profiles in benign and malignant prostate tissue. As with previous cancer profiling studies[7–10], molecular classification of prostate cancer was one of the goals of this analysis. We used two distinct reference samples for comparative microarray analysis: NAP tissue from patients with prostate cancer, and prostate tissue from men without documented prostate pathology. By making direct comparisons against normal tissue counterparts, we took advantage of a 'subtractive' effect, which emphasized genes that consistently distinguished normal and neoplastic tissues.

Prostate tissues used in microarray analysis included 4 BPH samples, 8 NAP samples, 1 commercial pool of normal prostate tissue (from 19 individuals), 1 prostatitis sample, and 11 localized and 7 metastatic prostate-cancer samples. Three cell lines from metastatic prostate cancer (DU-145, LnCAP and PC3) were also profiled for gene expression. Twenty-eight additional prostate tissue specimens were profiled and the data included in the Supplementary Information (samples of 9 BPH, 1 NAP, 13 metastatic and 5 localized prostate cancers). Fluorescently labelled (Cy5) cDNA was prepared from total RNA from each experimental sample. A second distinguishable fluorescent dye (Cy3) was used to label the two reference samples used in this study: a pool of NAP from four independent patients with prostate cancer and a commercial pool of normal prostate tissues. A direct comparison between the NAP and commercial pools was also made and notable differences in gene expression were readily apparent (Fig. 1 and Supplementary Information).

In all, more than 80 cDNA microarrays were used to assess gene expression in four clinical states of prostate-derived tissues and two distinct reference pools of normal specimens. Figure 1 provides an overview of the variation in gene expression across the different tissue specimens analysed (the full data set and 28 further samples can be seen in the Supplementary Information). A hierarchical clustering algorithm was used to group genes and experimental samples on the basis of similarities of gene expression over all that were tested. Relationships between the experimental samples are summarized as dendrograms (Fig. 1a), in which the pattern and length of the branches reflect the relatedness of the samples. Benign conditions of the prostate, such as BPH and NAP, cluster separately from malignant prostate-cancer cell lines or tissues, regardless of the reference pool used. Within the prostate-cancer cluster, metastatic and clinically localized prostate cancer formed distinct subgroups.

Eisen matrix formats[11] of the variation in gene expression show clusters of coordinately expressed genes, highlighting relationships between specimens (black bars in Fig. 1b, c). For example, clusters B3 and C1 represent genes downregulated in both localized and metastatic prostate cancer (Fig. 1b, c). By contrast, clusters B6 and B4 highlight genes that are specifically up- or downregulated in metastatic prostate cancer, respectively (Fig. 1b). *IGFBP-5*, *DAN1*, *FAT* tumour suppressor and *RAB5A* are examples of genes that are downregulated specifically in metastatic prostate cancer and also have a proposed role in oncogenesis (magnified regions, Fig. 1b).

Similarly, cancer-related genes that are upregulated in metastatic prostate cancer include *MTA-1* (metastasis-associated 1), *MYBL2* and *FLS353* (preferentially expressed in colorectal cancer).

We used several methods of gene selection to create a more limited set of genes for future exploration. In one method (others can be found in the Supplementary Information), we computed *t*-statistics (of prostate cancer versus benign tissue) for each gene. First, the *t*-values were ranked by absolute magnitude, which takes into account the inter-sample variability in expression ratios. Second, they were ranked by the magnitude of the numerator of the test statistic, which is based on the biological difference in expression ratios and designated as 'effect size'. We examined a list of the genes with the 200 largest effect sizes and 200 largest *t*-values and a scatterplot of their values (see Supplementary Information Fig. 5) to identify candidate genes. Implementing this methodology on both reference-pool data sets yielded genes that included *HPN* (*hepsin*), *PIM1*, *LIM* (*ENIGMA*), *TIMP2*, *HEVIN*, *RIG* and *THBS1* (*thrombospondin-1*), among others. Several genes are covered in detail in the Supplementary Information.

Many of the genes identified in these 'focused' clusters have been implicated directly or indirectly as cancer biomarkers or mediators of carcinogenesis. For example, the tumour-suppressor gene *PTEN* was downregulated, whereas the proto-oncogene *MYC* was upregulated in our microarray analysis of prostate cancer (see ref. 1 and Supplementary Information). Likewise, we observed decreased expression of *CDH1* (*E-cadherin*) and increased expression of fatty acid synthase, both of which have been shown to be dysregulated in prostate cancer[12,13]. In addition to uncharacterized expressed sequence tags (ESTs), numerous genes were identified by our screen but not previously known to be associated with prostate cancer. Furthermore, we assessed the data by examining functional

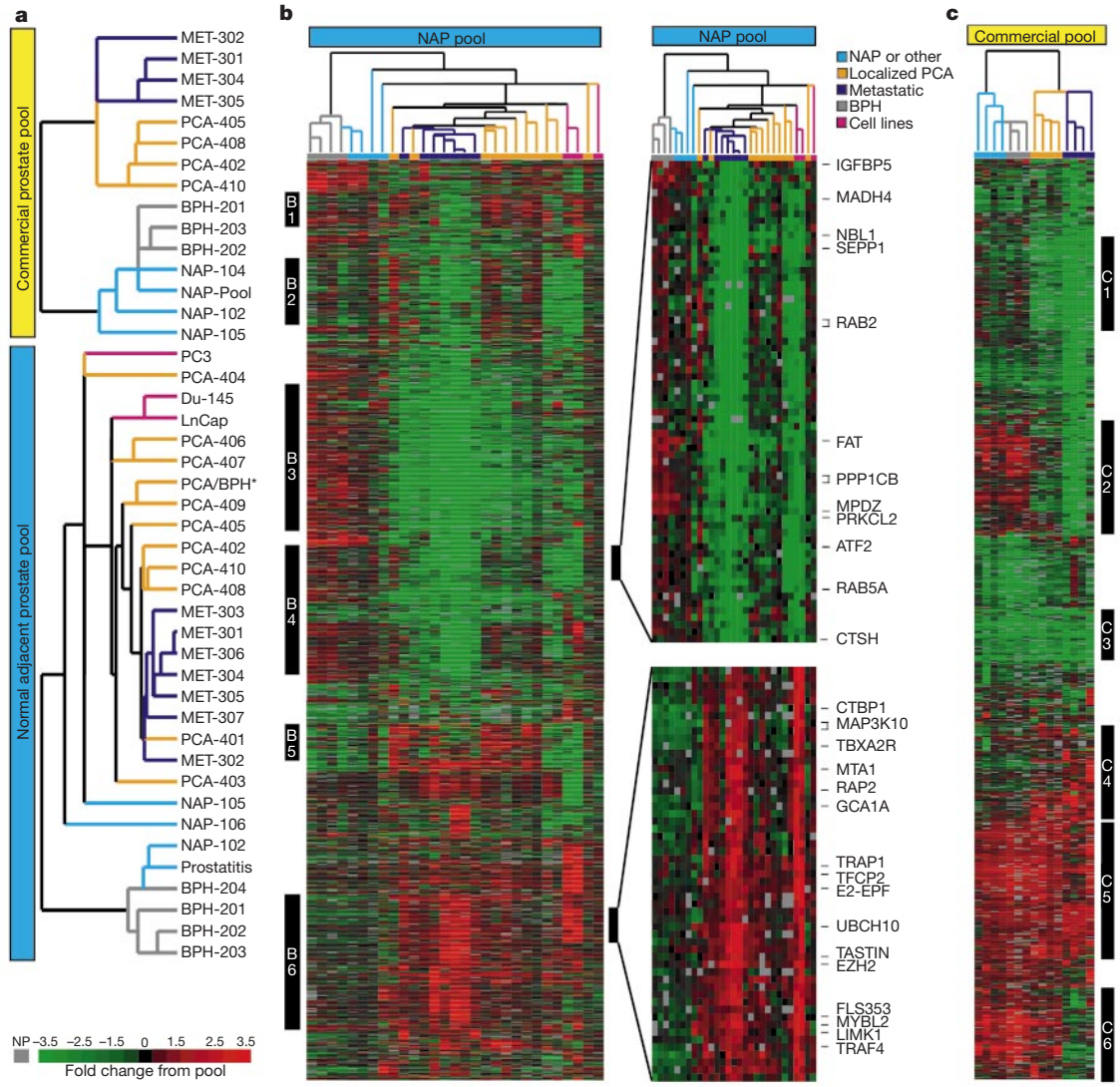

Figure 1 The molecular signature of prostate cancer. Gene-expression profiles of 44 experimental samples were performed using two distinct normal prostate reference pools (NAP pool and commercial pool). Samples analysed included NAP, localized (PCA) and metastatic (MET) prostate cancer, BPH, three prostate-cancer cell lines (DU-145, LnCAP and PC3) and prostatitis. **a**, Dendrograms reveal the variation in gene-expression pattern between experimental samples in the two pools. Asterisk indicates a sample that was initially documented as BPH, but later confirmed to have 5% cancer tissue. **b**, **c**, Cluster diagrams of the sample groups compared with the pool of normal adjacent prostate (**b**) or of commercial prostate (**c**). This clustering identifies distinct patterns of gene expression among the groups. Each row represents a single gene (1,520 genes in **b**, and 1,006 genes in **c**). Data are the quotient of hybridization of the fluorescent cDNA probe prepared from each experimental messenger RNA to its reference pool, and are a measure of relative gene expression in each sample. Red and green represent up- and downregulation, respectively (see scale in lower left corner), relative to the median of the pool. Grey signifies technically inadequate or missing data (NP, not present). Black bars on the sides (B1–B6 and C1–C6) indicate regions with characteristic gene expression signatures. Enlarged sections of B4 and B6 show selected genes. See Supplementary Information for full data sets.

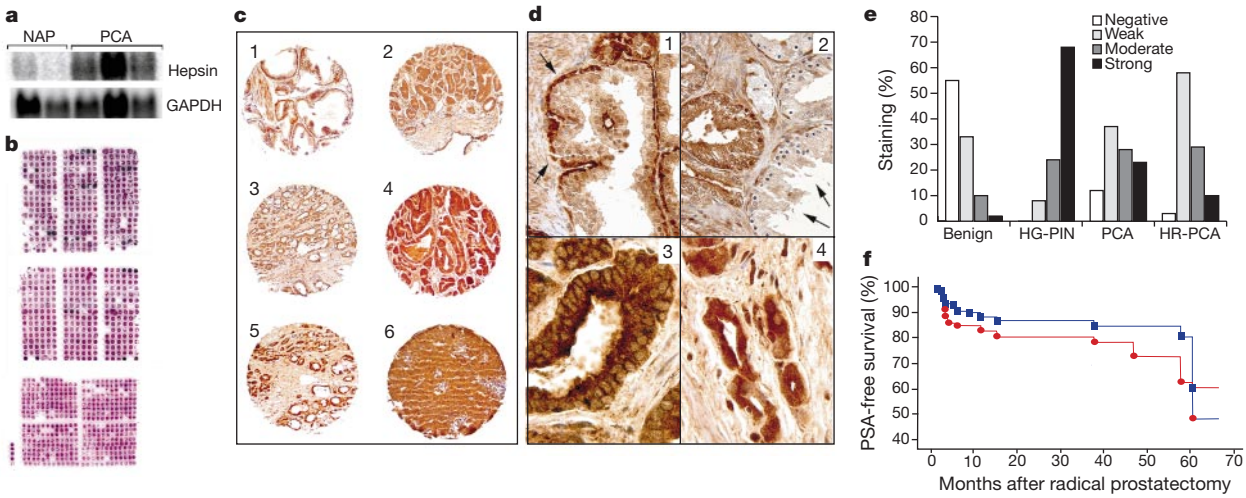

Figure 2 Hepsin is overexpressed in prostate cancer. **a**, Northern blot analysis of human hepsin and normalization with GAPDH. PCA, localized prostate cancer. **b**, Tissue microarrays used for hepsin analysis (stained with haematoxylin and eosin). **c**, Representative elements of a tissue microarray stained with anti-hepsin antibody. Immunohistochemical stains demonstrate absent or weak staining of benign prostate (c1), and strong staining in localized prostate cancer (c2–6). Magnification ×100. **d**, Benign prostate glands demonstrate strong basal cell staining (d1, arrows) but weak expression in the secretory luminal cells (d2, arrows). Where prostate cancer and benign prostate glands are seen (d2), marked differences in hepsin staining are observed. Infiltrating prostate cancers (d3 and d4) demonstrate strong expression of hepsin. Magnification ×400. **e**, Histogram of hepsin expression by tissue type. The relative strength of hepsin staining was assessed qualitatively (see text). HR-PCA, hormone refractory prostate cancer. **f**, Kaplan–Meier analysis. PSA-free survival was stratified by level of hepsin expression into two categories: absent or low (circles), and moderate or strong (squares).

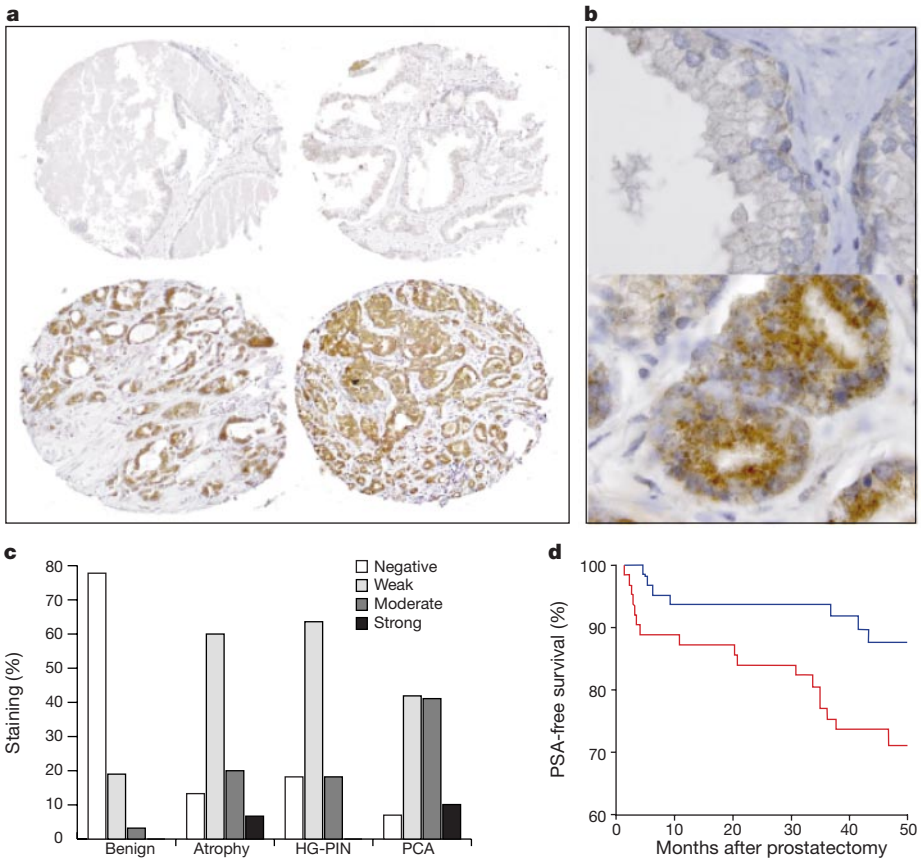

Figure 3 PIM1 is overexpressed in prostate cancer. **a**, Representative elements of a tissue microarray stained with anti-PIM1 antibody. Staining is absent or weak in benign prostate (top), but strong in the cytoplasm of localized prostate cancer (bottom). Magnification ×200. **b**, PIM1 expression is absent or weak in the secretory luminal cells of benign prostate glands (top), but strong in infiltrating prostate cancers (bottom). Magnification ×1,000. **c**, PIM1 protein expression by tissue type as assessed from 810 tissue-microarray elements. **d**, Kaplan–Meier analysis shows that patients with prostate cancer that have negative or weak PIM1 expression (red) are at a greater risk of developing PSA failure after prostatectomy than those that have moderate or strong expression (blue) (log-rank test, $P = 0.04$).

groups of known, named genes (see Supplementary Information).

Selected genes identified by microarray analysis were corroborated by northern analysis. For example, hevin, four and a half LIM domain protein and gelsolin were shown to be 3.2-, 3.2- and 1.9-fold downregulated, respectively, by microarray and 8.8-, 4.5- and 3.5-fold downregulated by northern analysis (data not shown). Similarly, hepsin was 4.3-fold upregulated by microarray and 11.3-fold upregulated by northern analysis (Fig. 2a). As hepsin is a cell-surface serine protease with transcript expression precisely restricted to localized and metastatic prostate cancer, we chose to examine its expression in more detail at the protein level.

We used a method for evaluating tumour tissues in large numbers on a single glass slide[14]. Sections of the microarrays of prostate-cancer tissue[15] used in this study are shown stained with haematoxylin and eosin in Fig. 2b. Hepsin immunohistochemistry was performed on three tissue microarrays containing a total of 738 specimens (Fig. 2c–e) using an affinity-purified hepsin-peptide antibody[16]. These samples included benign prostate tissue, BPH, high-grade prostatic intra-epithelial neoplasia (HG-PIN), and localized and metastatic prostate-cancer samples. Overall, hepsin exhibited staining predominantly in the plasma membrane and was preferentially expressed in neoplastic prostate over benign prostate (Mann–Whitney *U*-test, $P < 0.0001$). Importantly, the precursor lesion of prostate cancer, HG-PIN, had the strongest expression of hepsin, and almost never lacked staining (Mann–Whitney *U*-test, $P < 0.0001$). Most cases of low or absent hepsin staining were seen in benign prostate specimens (Fig. 2e). Interestingly, hormone-refractory metastatic cancers were intermediate in staining intensity between localized prostate tumours and benign prostate.

Men who develop elevated PSA levels following radical prostatectomy are at a high risk to develop distant metastases and die because of prostate cancer (termed PSA failure)[17]. Therefore to assess the usefulness of hepsin as a potential prostate-cancer biomarker, PSA failure was defined as a PSA elevation of greater than 0.2 ng ml^{-1} following radical prostatectomy. Outcomes analysis was performed on like-treated cases, and therefore was restricted to the 334 prostate-cancer samples from 78 men with clinically localized prostate cancer (each patient's tumour is replicated on average four times). The analysis was performed on 334 samples of localized prostate cancer, treating each as an independent sample. PSA elevation following radical prostatectomy was significantly associated with absent or low hepsin immunostaining, (Fig. 2f; log-rank test, $P = 0.03$).

Multivariate analysis was performed to examine whether these results were independent of the Gleason score, a well established histological grading system for prostate cancer[18]. Fitting a Cox proportional hazards model indicates an association of weak or absent hepsin protein expression in prostate cancer with increased risk of PSA elevation following prostatectomy, similar to having a high Gleason score (corresponding hazard ratios (HRs) were 2.9 ($P = 0.0004$) and 1.65 ($P = 0.037$), respectively). Weak or absent hepsin expression was also associated with large prostate cancers: the median tumour dimension for prostate tumours with moderate or strong expression was 1.3 cm but 1.5 cm for tumours with absent or weak staining (Mann–Whitney *U*-test, $P = 0.043$). Taken together, expression of hepsin protein in prostate cancer correlated inversely with measures of patient prognosis.

It is well known that the oncogene *MYC* is overexpressed in prostate cancer[1,19]; we demonstrate here that the protein kinase encoded by the proto-oncogene *PIM1* is similarly upregulated (Supplementary Information Fig. 7). Our analysis supports a remarkably similar co-transcriptional regulation (or gene amplification) of *PIM1* and *MYC*, possibly mediating a synergistic oncogenic effect in prostate cancer. Similar to hepsin, we explored expression of the protein PIM1 kinase in prostate cancer using high-density tissue microarrays. No or weak PIM1 expression was observed in most benign prostatic epithelial (97%), prostatic atrophy (73%) and HG-PIN (82%) samples (Fig. 3a–c). In contrast, moderate to strong PIM1 expression was observed in approximately half of the prostate cancer samples (51%; Fig. 3c). Kaplan–Meier analysis for PSA-free survival demonstrated that positive extraprostatic extensions, seminal vesicle invasions, Gleason scores greater than seven and decreased PIM1 expression were associated with a higher cumulative rate of PSA failure (Fig. 3d). By univariate Cox models, PIM1 expression is a strong predictor of PSA recurrence (HR = 2.1 (95% confidence interval 1.2–3.8), $P = 0.01$). Among the variables examined, significant predictors of PSA recurrence were Gleason score (HR = 1.8 (1.1–3.0), $P = 0.03$), Gleason pattern 4/5 prostate cancer (HR = 3.9 (1.8–8.3), $P < 0.001$), extraprostatic extension status (HR = 2.6 (1.6–4.2), $P < 0.0001$), surgical margin status (HR = 2.6 (1.2–5.6), $P = 0.01$), seminal vesicle status (HR = 3.5 (2.0–6.2), $P < 0.0001$), the natural log of pre-operative PSA level (HR = 2.5 (1.6–3.8), $P < 0.001$), and maximum tumour dimension (HR = 2.7 (1.6–4.7), $P < 0.0001$). By a multivariate Cox model, significant predictors of PSA recurrence were the presence of Gleason grades 4 and 5 prostate cancer (HR = 3.8 (1.4–10.0), $P < 0.01$), the natural log of pre-operative PSA level (HR = 2.1 (1.1–3.9), $P = 0.02$), and decreased PIM1 expression (HR = 4.5 (1.6–15.2), $P = 0.01$). Thus, even more so than hepsin, decreased expression of PIM1 kinase in prostate cancer correlated significantly with measures of poor patient outcome.

Analysis of the differential gene-expression profiles of normal and neoplastic prostate has identified a select set of genes that define a molecular signature for prostate cancer. By making direct comparative hybridizations of normal and neoplastic tissues, we emphasized genes that molecularly distinguish benign tissue from malignant—possibly accounting for the abundance of cancer-related genes picked up by our screen. Combining tissue microarrays, cDNA microarrays, and linked clinical and pathology data will facilitate rapid characterization of candidate biomarkers and regulatory cancer genes, as demonstrated here with respect to hepsin and PIM1 kinase. □

Methods

Preparation of total RNA and reference pools

The prostate surgical specimens were obtained from The University of Michigan Specialized Research Program in Prostate Cancer (SPORE) tumour bank with Institutional Review Board approval. Tissues were homogenized in Trizol (Gibco) and the total RNA was isolated according to the standard Trizol protocol. Total RNA integrity was judged by denaturing-formaldehyde agarose gel electrophoresis. Total RNA from four normal tissues was combined in equal concentrations to obtain the reference pool. The human prostate total RNA used in the commercial reference pool was obtained from Clontech.

Microarray procedures

Complementary DNA microarray analysis of gene expression was done essentially as described (available at http://www.microarrays.org). The sequence-verified cDNA clones on the human cDNA microarray are listed in the Supplementary Information and are available from the Research Genetics web site (http://www.resgen.com). Based on the latest build of Unigene, our 10K human cDNA micorarray covers about 5,520 known, named genes and 4,464 ESTs. Protocols for printing and post-processing of arrays are available (http://www.microarrays.org/protocols.html).

Data analysis

Primary analysis was done with the Genepix software package. Cy3-to-Cy5 ratios are determined for the individual genes along with various other quality-control parameters (for example, intensity over local background). Furthermore, bad spots or areas of the array with obvious defects were manually flagged. Flagged spots were not included in subsequent analyses.

These files were then imported into a Microsoft Access database. Before clustering, the normalized median of ratio values of the genes were $\log_2$ transformed, filtered for presence across arrays, and selected for expression levels and patterns depending on the experimental set as stated in the figure legends. Average-linkage hierarchial clustering of an uncentred Pearson correlation similarity matrix was applied with the program Cluster[11], and the results were analysed; figures were generated with the program TreeView. Before hierarchical clustering, the data were filtered for at least a twofold change in expression ratio and ratio measurements present in 50% of the samples, thus yielding 1,520 genes from the NAP data set (Fig. 1b). Similarly, a threefold change with 75% measurements present yielded 1,006 genes from the commercial pool (Fig. 1c) data set.

Northern blot analysis

Thirty micrograms of total RNA were resolved by denaturing-formaldehyde agarose gel and transferred onto Hybond membrane (Amersham). The signal was visualized and quantified by phosphorimaging. For relative fold estimation, the ratio between the signals obtained from hepsin and GAPDH probes was calculated. For northern analysis, we compared the intensity of the transcript (as determined by phosphorimaging) in NAP tissue with that of localized prostate cancer. The results are first normalized against a GAPDH control and a ratio of cancer to normal is then obtained. Similarly, for microarray analysis, the normalized Cy5/Cy3 quotient of normal tissue is compared to the Cy5/Cy3 quotient of prostate cancer and a ratio of cancer to normal tissue is obtained.

Immunohistochemistry and tissue microarrays

High-density tissue microarrays were assembled as previously described[14,15]. Initial sections were stained for haematoxylin and eosin to verify histology. Standard biotin–avidin-complex immunohistochemistry was performed. The affinity-purified polyclonal rabbit antibody against hepsin was used at a 1:40 dilution (original concentration 0.2 mg ml^{-1}) for this study. Immunostaining intensity was scored by a genito-urinary pathologist (M.A.R.) as absent, weak, moderate or strong. Scoring was performed blind using a telepathology system without knowledge of overall Gleason score (for example, tumour grade), tumour size or clinical outcome[15]. A total of 738 tissue samples from benign (n = 205), HG-PIN (n = 38), localized prostate cancer (n = 335) and metastatic prostate cancer (n = 160) were examined.

Similarly, PIM1 was analysed using two tissue-microarray blocks from 810 prostate-cancer samples from 135 patients. Six prostate-cancer samples were evaluated from each case and a median score was calculated. In addition, a few samples with benign prostatic tissues (for example, benign epithelium and atrophy) and HG-PIN were examined. Immunohistochemistry was performed as above, using a rabbit polyclonal antibody against the carboxy terminus of PIM1 (Santa Cruz Biotechnology) at a dilution of 1:100.

Case selection

Cases of clinically localized prostate cancer were identified from the University of Michigan Prostate SPORE tumour bank. The advanced prostate tumours were collected from a series of rapid autopsies performed at the University of Michigan on men who died of metastatic prostate cancer. Autopsies were performed 4–6 h after death. The clinical and pathologic findings of these cases have recently been reported[20].

Statistical methods

A nonparametric analysis of variance test (Mann–Whitney, two categories) was used to evaluate whether the prostate samples expressed hepsin and PIM1 at different levels based on various parameters (tissue type, Gleason score and tumour size). Kaplan–Meier analysis was used to estimate the cumulative percentage of PSA-free progression ('survival'). The log-rank test was used to assess the differences in disease-free progression hepsin immunostaining. Cox proportional-hazard regression was used for multivariate analyses.

Received 16 January; accepted 26 June 2001.

1. Abate-Shen, C. & Shen, M. M. Molecular genetics of prostate cancer. *Genes Dev.* **14,** 2410–2434 (2000).
2. Ruijter, E. *et al.* Molecular genetics and epidemiology of prostate carcinoma. *Endocr. Rev.* **20,** 22–45 (1999).
3. Barry, M. J. Prostate-specific-antigen testing for early diagnosis of prostate cancer. *N. Engl. J. Med.* **344,** 1373–1377 (2001).
4. Liotta, L. & Petricoin, E. Molecular profiling of human cancer. *Nature Rev. Genet.* **1,** 48–56 (2000).
5. Elek, J., Park, K. H. & Narayanan, R. Microarray-based expression profiling in prostate tumors. *In Vivo* **14,** 173–182 (2000).
6. Emmert-Buck, M. R. *et al.* Molecular profiling of clinical tissue specimens: feasibility and applications. *Am. J. Pathol.* **156,** 1109–1115 (2000).
7. Golub, T. R. *et al.* Molecular classification of cancer: class discovery and class prediction by gene expression monitoring. *Science* **286,** 531–537 (1999).
8. Bittner, M. *et al.* Molecular classification of cutaneous malignant melanoma by gene expression profiling. *Nature* **406,** 536–540 (2000).
9. Perou, C. M. *et al.* Molecular portraits of human breast tumours. *Nature* **406,** 747–752 (2000).
10. Alizadeh, A. A. *et al.* Distinct types of diffuse large B-cell lymphoma identified by gene expression profiling. *Nature* **403,** 503–511 (2000).
11. Eisen, M. B., Spellman, P. T., Brown, P. O. & Botstein, D. Cluster analysis and display of genome-wide expression patterns. *Proc. Natl Acad. Sci. USA* **95,** 14863–14868 (1998).
12. Tomita, K. *et al.* Cadherin switching in human prostate cancer progression. *Cancer Res.* **60,** 3650–3654 (2000).
13. Shurbaji, M. S., Kalbfleisch, J. H. & Thurmond, T. S. Immunohistochemical detection of a fatty acid synthase (OA-519) as a predictor of progression of prostate cancer. *Hum. Pathol.* **27,** 917–921 (1996).
14. Kononen, J. *et al.* Tissue microarrays for high-throughput molecular profiling of tumor specimens. *Nature Med.* **4,** 844–847 (1998).
15. Perrone, E. E. *et al.* Tissue microarray assessment of prostate cancer tumor proliferation in African-American and white men. *J. Natl Cancer. Inst.* **92,** 937–939 (2000).
16. Tsuji, A. *et al.* Hepsin, a cell membrane-associated protease. Characterization, tissue distribution, and gene localization. *J. Biol. Chem.* **266,** 16948–16953 (1991).
17. Pound, C. R. *et al.* Natural history of progression after PSA elevation following radical prostatectomy. *Jama* **281,** 1591–1597 (1999).
18. Gleason, D. F. Histologic grading of prostate cancer: a perspective. *Hum. Pathol.* **23,** 273–279 (1992).
19. Buttyan, R., Sawczuk, I. S., Benson, M. C., Siegal, J. D. & Olsson, C. A. Enhanced expression of the c-myc protooncogene in high-grade human prostate cancers. *Prostate* **11,** 327–337 (1987).
20. Rubin, M. A. *et al.* Rapid ('warm') autopsy study for procurement of metastatic prostate cancer. *Clin. Cancer Res.* **6,** 1036–10345 (2000).

Supplementary information is available on *Nature*'s World-Wide Web site (http://www.nature.com) or as paper copy from the London editorial office of *Nature*.

Acknowledgements

We are indebted to P. Ward and the University of Michigan Microarray Network for support and encouragement in the development of the Pathology Microarray Node. We thank M. Sanda and J. Wei for support of the clinical database; E. Cushenberry for her help with collecting the prostate tissue samples, The University of Michigan Comprehensive Cancer Center Histology and Immunoperoxidase Core; and the instructors of the 1999 Cold Spring Harbor Workshop on DNA Microarrays. This work is supported by developmental grants (A.M.C. and M.A.R.) from the Specialized Program of Research Excellence in Prostate Cancer, National Cancer Institute.

Correspondence and requests for materials should be addressed to A.M.C. (e-mail: arul@umich.edu).

Haematopoietic cell-specific CDM family protein DOCK2 is essential for lymphocyte migration

Yoshinori Fukui*, Osamu Hashimoto*†, Terukazu Sanui*, Takamasa Oono*, Hironori Koga†, Masaaki Abe‡, Ayumi Inayoshi*, Mayuko Noda*, Masahiro Oike§, Toshikazu Shirai‡ & Takehiko Sasazuki*‖

* *Division of Immunogenetics, Department of Immunobiology and Neuroscience, Medical Institute of Bioregulation, Kyushu University, and CREST, Japan Science and Technology Corporation, 3-1-1 Maidashi, Higashi-ku, Fukuoka 812-8582, Japan*

† *Research Center for Innovative Cancer Therapy, Kurume University School of Medicine, Asahimachi 67, Kurume 830-0011, Japan*

‡ *The Second Department of Pathology, Juntendo University School of Medicine, 2-1-1 Hongo, Bunkyo-ku, Tokyo 113-0033, Japan*

§ *Department of Pharmacology, Graduate School of Medical Sciences, Kyushu University, 3-1-1 Maidashi, Higashi-ku, Fukuoka 812-8582, Japan*

‖ *International Medical Center of Japan, 1-12-1 Toyama, Shinjuku-ku, Tokyo 162-8655, Japan*

Cell migration is a fundamental biological process involving membrane polarization and cytoskeletal dynamics[1], both of which are regulated by Rho family GTPases[2–5]. Among these molecules, Rac is crucial for generating the actin-rich lamellipodial protrusion, a principal part of the driving force for movement[3,6]. The CDM family proteins, *Caenorhabditis elegans* CED-5, human DOCK180 and *Drosophila melanogaster* Myoblast City (MBC), are implicated to mediate membrane extension by functioning upstream of Rac[7–12]. Although genetic analysis has shown that CED-5 and Myoblast City are crucial for migration of particular types of cells[8,9,12], physiological relevance of the CDM family proteins in mammals remains unknown. Here we show that DOCK2, a haematopoietic cell-specific CDM family protein[13], is indispensable for lymphocyte chemotaxis. DOCK2-deficient mice (DOCK2$^{-/-}$) exhibited migration defects of T and B lymphocytes, but not of monocytes, in response to chemokines, resulting in several abnormalities including T lymphocytopenia, atrophy of lymphoid follicles and loss of marginal-zone B cells. In DOCK2$^{-/-}$ lymphocytes, chemokine-induced Rac activation and actin poly-